

RESEARCH

Open Access



Identification of CENPW as a prognostic biomarker and potential therapeutic target for clear cell renal cell carcinoma

Haibing Xiao^{1,2*}, Qili Xu^{1,2†}, Yu Gao^{1,2†}, Weikang Wu^{1,2}, Baojun Wang^{1,2}, Haolin Li^{3*} and Mintian Fei^{1,2*}

[†]Haibing Xiao, Qili Xu and Yu Gao have contributed equally to this work.

*Correspondence:

Haibing Xiao
xiaohaibing@ahmu.edu.cn
Haolin Li
cnli_haolin@outlook.com
Mintian Fei
mintianfei2022@163.com

¹Department of Urology, The First Affiliated Hospital of Anhui Medical University, Hefei, Anhui, People's Republic of China

²Anhui Province Key Laboratory of Urological and Andrological Diseases Research and Medical Transformation, Anhui Medical University, Hefei, Anhui, People's Republic of China

³Department of Urology, The 1st Affiliated Hospital of Kunming Medical University, Kunming 650032, China

Abstract

Centromere protein W (CENP-W) is essential for chromosome segregation and mitotic assembly and has been recognized as a prognostic marker in several cancers. However, its significance in clear-cell renal cell carcinoma (ccRCC) remains underexplored. To investigate this, we analyzed transcriptomic data from the National Center for Biotechnology Information (NCBI) and The Cancer Genome Atlas (TCGA) to evaluate CENP-W expression and its associations with clinical outcomes, prognosis, and immune-related markers. Kaplan–Meier survival analysis indicated that elevated CENP-W levels are significantly associated with poorer overall survival in ccRCC patients. Further meta- and multivariate analyses confirmed CENP-W as an independent negative prognostic factor. Gene Set Enrichment Analysis (GSEA) revealed the involvement of CENP-W in immune-related pathways, notably PI3K-Akt and Wnt signaling. Pearson correlation analysis revealed strong associations between CENP-W expression and immune cell infiltration, cancer-associated fibroblasts (CAFs), CTLA4, and PDCD1. qRT-PCR assays confirmed elevated CENP-W levels in ccRCC samples. Additionally, GSEA and GO enrichment highlighted a relationship between CENP-W and lipid metabolism, with reduced CENP-W expression leading to a significant decrease in lipid droplet accumulation. This study identifies CENP-W as a potential biomarker and prognostic indicator in ccRCC, offering insights into personalized therapeutic strategies integrating tumor immunity to enhance the efficacy of immunotherapy.

Highlights

1. Renal cancer is often late, making early diagnosis crucial.
2. CENPW is highly expressed in tumor and is associated with poor prognosis.
3. CENPW is related to tumor immune infiltration.
4. The link between CENPW, immune checkpoints, and immunotherapy was examined.

Keywords ccRCC, CENPW, Immune checkpoint, Lipid metabolism



1 Introduction

Renal cell carcinoma (RCC) is a heterogeneous malignancy that originates from the renal tubular epithelial cell and accounts for about 90 percent of kidney cancers [1]. It is one of the ten most common cancers globally, with epidemiological statistics showing that there are more than 400,000 new cases each year [2], and the incidence is higher in men than in women [3]. Clear cell renal cell carcinoma (ccRCC) is the predominant subtype of renal cell carcinoma (RCC), representing approximately 70%–80% of cases. Papillary renal cell carcinoma (pRCC) and chromophobe renal cell carcinoma (chRCC) rank as the second and third most prevalent subtypes of renal cell cancer, respectively, comprising about 10–15% and 3–5% of RCC cases, respectively.[4]

CENPW, located on chromosome 6q22.32 [5], contains a 267 bp open reading frame and is regulated by its upstream promoter region [6], resulting in the transcription of a 600 bp mRNA. Also known as cancer upregulated gene 2 (CUG2), expression of CENPW has been found to be significantly increased in certain malignancies, such as cervical, colon, liver, and lung cancers [7–10]. Current research identifies CENPW as a critical component of the kinetochore, where it stabilizes the pre-assembly complex, thereby ensuring the proper progression of mitosis [11]. This stabilization is pivotal in regulating the cell cycle and promoting tumor cell proliferation [12]. Additionally, CENPW has been shown to significantly influence the migratory and invasive capabilities of hepatocellular carcinoma cells, underscoring its potential as a predictive biomarker for this type of cancer [13].

Immune checkpoints represent a key mechanism by which tumor cells evade attacks from the immune system [14]. Tumor cells primarily achieve this by inhibiting T cell activity, thereby reducing the immune system's ability to recognize and target them. The most significant immune checkpoint pathways currently identified are the PD-1/PD-L1 axis and CTLA-4 [15]. Ongoing research into immune checkpoint molecules and combination therapies continues to yield novel strategies aimed at improving cancer treatment outcomes [16].

2 Materials and methods

2.1 Data sources

Relating data were collected from TCIA (The Cancer Immunome Atlas; <https://tcia.at/home>); The Cancer Genome Atlas (TCGA, <https://portal.gdc.cancer.gov/>); The Gene Expression Omnibus (GEO, <https://www.ncbi.nlm.nih.gov/geo/>); The Gene Expression Profiling Interactive Analysis (GEPIA, <https://gepia.cancer-pku.cn/>); Tumor Immune Estimation Resource (TIMER, <https://cistrome.shinyapps.io/timer/>); STRING (<https://cn.string-db.org/>).

2.2 Human samples

Tissue samples, comprising ccRCC and non-tumor tissues, were procured from the Department of Urology at the First Affiliated Hospital of Anhui Medical University, during 2022–2023 years. Pathological diagnosis confirmed the tumor type of each sample, and informed consents were acquired from all patients. The present investigation implemented the guidelines outlined in the Declaration of Helsinki and received approval from the Ethics Committee of Human Research at the First Affiliated Hospital of Anhui Medical University (PJ2024-11-95).

2.3 Cell culture and reagents

All cell lines used in this study were obtained from Procell (Wuhan, China). Cultures were maintained under standard conditions at 37 °C with 5% CO₂. The specific growth media for each cell line were as follows: CAKI-1 cells were cultured in McCoy's 5A medium with 10% FBS; A-498 and ACHN cells were cultured in MEM medium with 10% FBS; 786-O and OS-RC-2 cells were cultured in RPMI 1640 medium supplemented with 10% fetal bovine serum (FBS). Additionally, the HK-2 human proximal tubular cell line was cultured in MEM medium with 10% FBS, and human embryonic kidney (HEK) 293-T cells were maintained in high-glucose DMEM medium supplemented with 10% FBS.

2.4 Real-time quantitative PCR

It is common to use TRIzol reagent (Invitrogen, Carlsbad, CA) to extract RNA from cells and tissues. First, samples are washed three times with PBS, after adding TRIzol, let samples dissolve at room temperature for 15 min. Then samples are centrifuged using a high-speed centrifuge. Next, mRNA is extracted using chloroform, and after centrifugation, the upper aqueous phase is discarded while the lower precipitate is retained. The precipitate is then washed and purified with anhydrous ethanol. Finally, the RNA is dissolved in DEPC-treated water, and its purity and concentrations are measured using a spectrophotometer. For cDNA synthesis, mRNA extracted by this method is reverse transcribed using the PrimeScript™ RT Reagent Kit (Takara, Japan) according to the manufacturer's instructions. The cDNA was amplified using SYBR Green Master Mix (Takara, Japan), and mRNA levels in cells or tissues were quantified on the ABI7500 platform (Thermo Fisher Scientific, USA). The primers used are:

GAPDH:

F: 5'-TTGCCCTCAACGACCACTTT-3'

R: 5'-TGGTCCAGGGGTCTTACTCC-3'

CENPW:

F: 5'-AAGCCTCAACTTCGTCTGGAG-3'

R: 5'-CACAAGCGTTTGTCTGGACT-3'

2.4.1 Cell migration and invasion assay

The 786-O and CAKI-1 cells treated with si-CENPW were trypsinized, centrifuged, and then resuspended in a medium devoid of serum. The cells were subsequently seeded into the upper chambers of transwell inserts at densities of 3,000 cells/mL for migration assays and 5000 cells/mL for invasion assays. Following 36 h of incubation at 37 °C in a 5% CO₂ atmosphere, the cells were treated with 4% formaldehyde, using crystal violet for staining. Cell counts were then quantified under a microscope.

2.5 Cell proliferation assay

786-O and CAKI-1 cells treated with sh-RNA were seeded into 96-well plates at a density of 2000 cells/mL. After the cells adhered, cell proliferation was assessed at 0, 1, 2, 3, and 4 days using the Cell Counting Kit-8 (GlpBio, #GK10001). Absorbance was measured at a wavelength of 450 nm using a microplate reader.

2.6 Oil red O staining assay

Seeded onto six-well plates, cells were evaluated for lipid droplet concentration after reaching 70% confluence using the Oil Red O Stain Kit (Solarbio, G1262). The cells were first washed twice with PBS and then fixed with a fixing buffer for 30 min. After two rinses with distilled water, the cells were incubated in 60% isopropanol for 5 min. Freshly prepared Oil Red O staining solution was applied for 20 min, followed by a 2-min incubation with Mayer's hematoxylin staining solution. The stain was discarded, using PBS to wash cells three times. The results were then documented using a microscope.

2.7 Lipid droplet staining and quantification

Lipid droplet detection was performed using BODIPY 493/503 (Invitrogen, #D2191). Cells were seeded into six-well plates, and when they reached 50% confluence, the detection was carried out. First, wash the cells twice with PBS, then fix them with 4% formaldehyde at room temperature for 20 min. Next, incubate the cells with 2 μ M BODIPY 493/503 at 37 °C in the dark for 15 min. Stain the cells with Hoechst 33342 (10 μ g/mL, MCE, HY-15559) for 5 min. Finally, use a fluorescence microscope to detect the lipid droplet content in the cells.

2.8 Statistical analysis

Statistical analysis was conducted with R-4.3.1 and GraphPad Prism 10.0. For statistical differences analysis, students' t-tests or ANOVA analyses were utilized.

3 Results

3.1 CENPW is abnormally upregulated in ccRCC

First, using the TIMER database, the authors investigated the changes in CENPW expression levels in cancer tissues compared to normal samples. The results showed that CENPW is significantly upregulated in most cancer types, including ccRCC (Fig. 1a, b). CENPW expression profiles from the GSE36895 and GSE53757 datasets also confirmed our conclusion (Fig. 1c, d). To further validate the results based on high-throughput sequencing and gene microarray, samples collected from clear cell renal cell carcinoma patients were subjected to an RT-qPCR experiment. There was a significant upregulation of CENPW mRNA expression in clear cell renal cell carcinoma tissues (Fig. 1e). A detailed statistical analysis of the sample characteristics used in these experiments is presented in Table 1.

3.2 High expression of CENPW is associated with clinical characteristics

The objective of this work is to investigate the role of CENPW in ccRCC pathogenesis by analyzing the correlation between CENPW expression and clinical features of ccRCC. Using the TCGA-KIRC dataset, authors identified that CENPW expression levels were significantly associated with T-stage, N-stage, M-stage, clinical stage, and patient's vital status but had no correlation with gender and age (Table 2). Furthermore, CENPW expression was elevated in advanced T-stage (Fig. 1f), N-stage (Fig. 1g), and M-stage (Fig. 1h). Additionally, high CENPW expression was associated with poorer histologic grade and clinical stage (Fig. 1i, j).

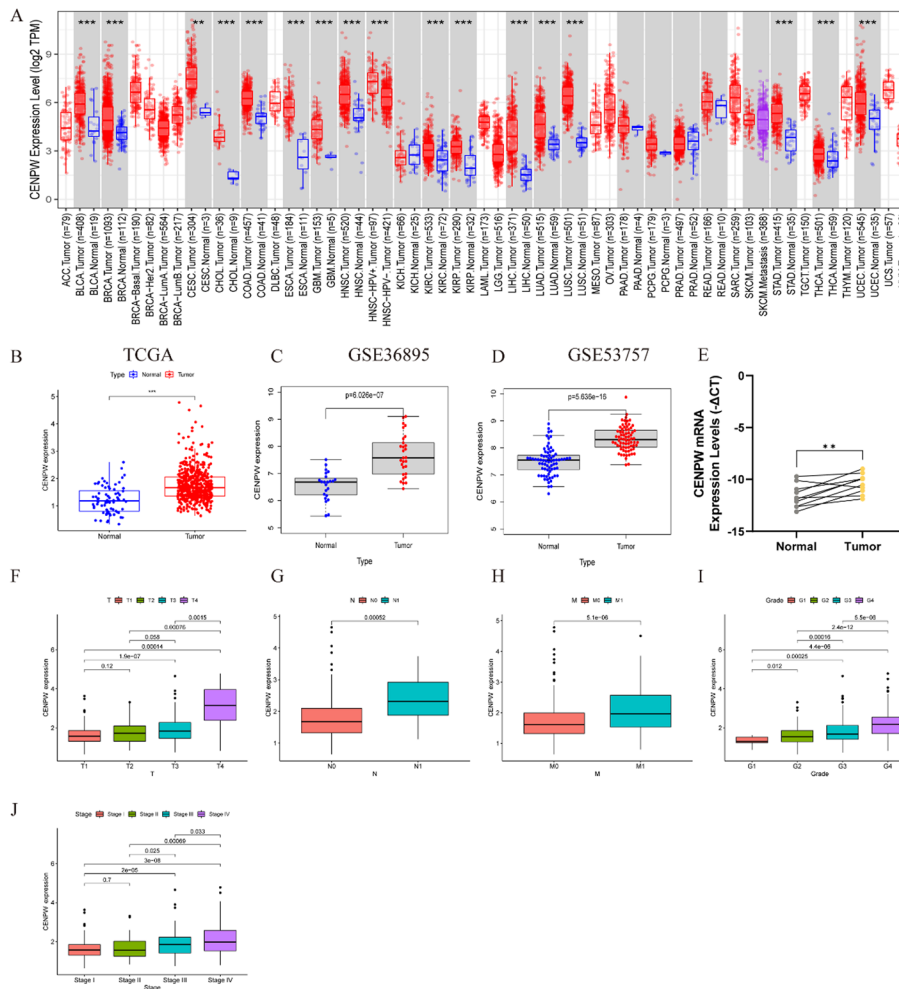


Fig. 1 The expression level of CENPW in ccRCC and normal tissues. **a** The expression level of CENPW in TCGA projects based on the TIMER2.0 database. **b-d** The expression changes of CENPW in TCGA-KIRC, GSE36895, and GSE53757 datasets. **e** The mRNA levels of CENPW in paired ccRCC patients' tissues. **f-j** The association of CENPW expression levels and clinical characteristics. * $P < 0.05$, ** $P < 0.01$, *** $P < 0.001$

Table 1 The samples information used in this study

	Pathological pattern	Gender	Age(y)	Position	Size	TNM
Case 1	ccRCC, Fuhrman 2	Male	59	Right	4.2×3.9×4.2 cm	T1bN0M0
Case 2	ccRCC, Fuhrman 2	Female	65	Right	12×4.0×4.0 cm	T2bN0M0
Case 3	ccRCC, Fuhrman 2	Male	57	Right	6×4.5×4.5 cm	T1bN0M0
Case 4	ccRCC, Fuhrman 2	Male	52	Left	10×9×9 cm	T2bN0M0
Case 5	ccRCC, Fuhrman 2	Male	68	Left	8×6×4 cm	T3bN1M0
Case 6	ccRCC, Fuhrman 2	Male	59	Left	5.5×5.0×4.5 cm	T1bN0M0
Case 7	ccRCC, Fuhrman 1–2	Male	61	Left	3.2×2.2×1.1 cm	T1aN0M0
Case 8	ccRCC, Fuhrman 2	Female	71	Left	3×3×2.5 cm	T1aN0M0
Case 9	ccRCC, Fuhrman 2	Male	64	Right	5.7×2.9×2.7 cm	T1bN0M0
Case 10	ccRCC, Fuhrman 2	Male	54	Right	5×4.5×4 cm	T1bN0M0

3.3 High expression of CENPW predicts poor clinical outcomes

From the above analysis, the authors demonstrated elevated CENPW expression in ccRCC and its correlation with clinical characteristics. However, whether CENPW is positively associated with ccRCC malignancy is still largely unknown. To address this,

Table 2 The characteristic of CENPW in clear cell renal cell carcinoma

Characteristic	Total (n=514)	CENPW		p Value
		High(257)	Low(257)	
Gender				
Male	330	169	161	0.5195
Female	184	88	96	
Age (median [IQR])	60.500 [52.000, 69.750]	60.000 [51.000, 69.000]	61.000 [52.000, 70.000]	0.2505
T				
T1	257	113	144	0.0066*
T2	66	30	36	
T3	180	106	74	
T4	11	8	3	
N				
N0+NX	498	244	254	0.0223*
N1	16	13	3	
M				
M0+MX	435	208	227	0.0277*
M1	79	49	30	
Stage				
I	251	109	142	0.0008*
II	54	21	33	
III	123	72	51	
IV	83	52	31	
Not report	3	3	0	
Grade				
1	13	4	9	0.0004*
2	217	95	122	
3	201	101	100	
4	75	54	21	
X	8	3	5	
Vital status				
Alive	357	159	198	0.0006*
Dead	154	97	57	
Not report	3	1	2	

the authors stratified patients into high and low CENPW expression groups based on the median CENPW expression level in the TCGA-KIRC dataset. Then Kaplan–Meier survival analysis was conducted, and the findings indicated that the high expression group had a notably lower overall survival rate compared to the low expression group (Fig. 2a), and the disease-free survival of the high expression group was markedly lower than that of the low expression group (Fig. 2b). To evaluate the predictive accuracy of CENPW for survival outcomes, the authors performed ROC curve analysis, which demonstrated that CENPW serves as an accurate diagnostic indicator for ccRCC patients (Fig. 2a, b). In order to confirm the reported findings, Cox regression analysis was employed to ascertain if CENPW was a risk factor for ccRCC patient outcomes. The results showed that in addition to Age, Grade, Stage, T-stage, and M-stage, CENPW was a significant risk factor for the prognosis of ccRCC patients (Fig. 2c). Multivariate analysis further identified CENPW as an independent adverse factor, with age, grade, and stage also contributing negatively to patient outcomes in the TCGA-KIRC dataset (Fig. 2d). Furthermore, three independent datasets validated that CENPW influenced prognosis for patients with ccRCC (Fig. 2e).

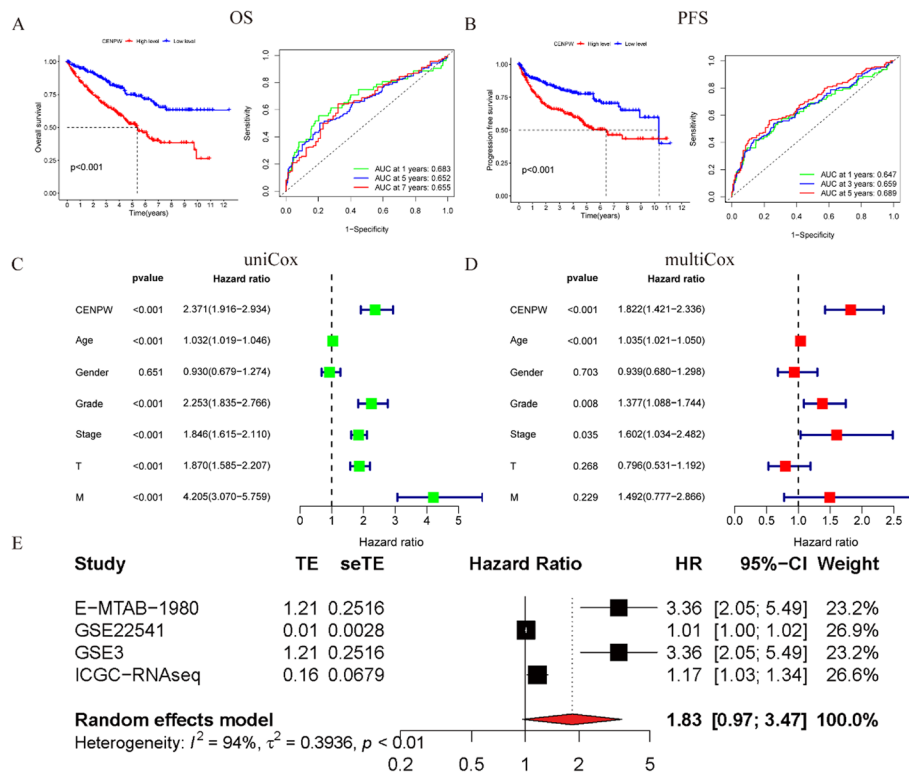


Fig. 2 The prognosis analysis of CENPW in the TCGA-KIRC dataset. **a** The overall survival and time-dependent ROC curves of 1-, 3-, and 5-year survival rates of ccRCC patients. The area under the curve (AUC) > 0.6 was considered as a threshold. **b** The disease-free survival and time-dependent ROC curves of 1-, 3-, and 5-year survival rates of ccRCC patients. The area under the curve (AUC) > 0.6 was considered as a threshold. **c** Univariate COX regression analysis on CENPW expression and other clinical characteristics of ccRCC. **d** Multivariate COX regression analysis on CENPW expression and other clinical characteristics of ccRCC. **e** The meta-analysis of CENPW prognostic value based on four independent datasets

3.4 Investigate the function of CENPW in ccRCC

Recognizing CENPW as a deleterious factor in ccRCC, this study further explored the potential signaling pathways in which CENPW may be involved. The authors first classified the data from the TCGA-KIRC dataset into high and low expression groups according to the median CENPW expression value. Comparative analysis of gene expression profiles between these groups revealed significant differences (Fig. 3a). Then, KEGG and Gene Ontology analysis were performed to identify the significant pathways enriched in these two groups. The results showed that several pathways often abnormally upregulated in malignancy, such as the PI3K-Akt and Wnt signaling pathways, were enriched (Fig. 3b). Interestingly, pathways related to lipid metabolism—such as cholesterol metabolism, high-density lipoprotein particle pathways, and fat digestion and absorption—were also enriched (Fig. 3b, c). High-density lipoprotein is the main carrier involved in cholesterol transport, which indicates that CENPW may be involved in cholesterol metabolism in ccRCC. The authors also found enriched cytokine-cytokine receptor interaction (Fig. 3b), B cell-mediated immunity, antigen binding, and immunoglobulin receptor binding (Fig. 3c) indicating that CENPW may impact immune cell infiltration and the tumor microenvironment in ccRCC. GSEA was also performed to complete GO and KEGG enrichment results. After analyzing the results, the authors found that CENPW may promote ccRCC development by activating the P53 signal pathway and

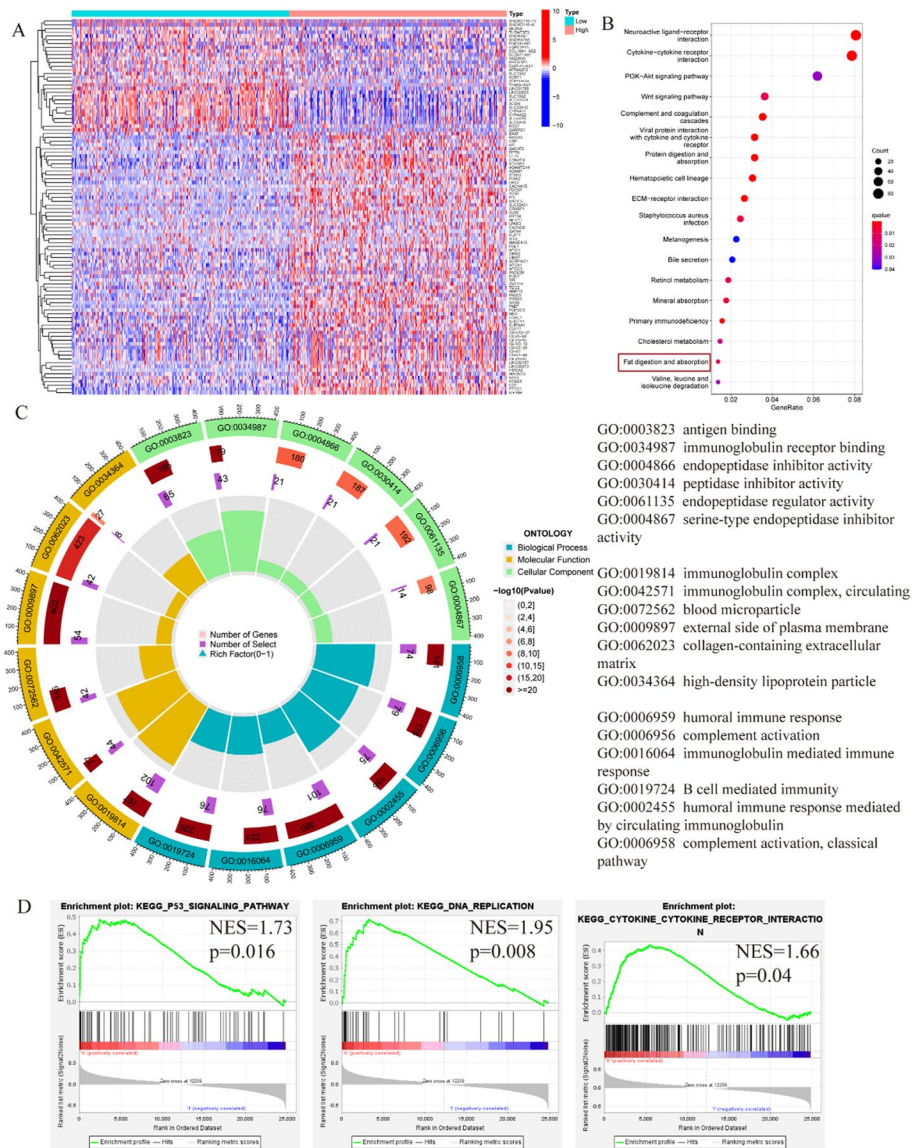


Fig. 3 Functional enrichment analysis of CENPW in ccRCC. **a** Different expression genes between high and low CENPW expression groups. **b** KEGG Enrichment analysis of CENPW in ccRCC. **c** GO enrichment analysis of CENPW in biological process (BP), molecular function (MF), and cellular component (CC). **d** Gene set enrichment analysis (GSEA) of CENPW in ccRCC

participating in DNA replication. The cytokine-cytokine receptor interaction pathway was significantly enriched in the high-CENPW expression group (Fig. 3d), which was consistent with KEGG enrichment results (Fig. 3b).

3.5 PPI network and co-expression analysis of CENPW

A protein–protein interaction (PPI) network was constructed using the STRING database (Fig. 4a). Then, Degree and Maximum Neighborhood Component (MNC) algorithms were carried out to recognize the hub genes from this network. The top 10 genes calculated by these two methods showed significant consistency (Fig. 4b). The GO enrichment of these hub genes showed that these genes were related to protein-DNA complex, chromosome, and kinetochore (Fig. 4c). These findings suggest that CENPW

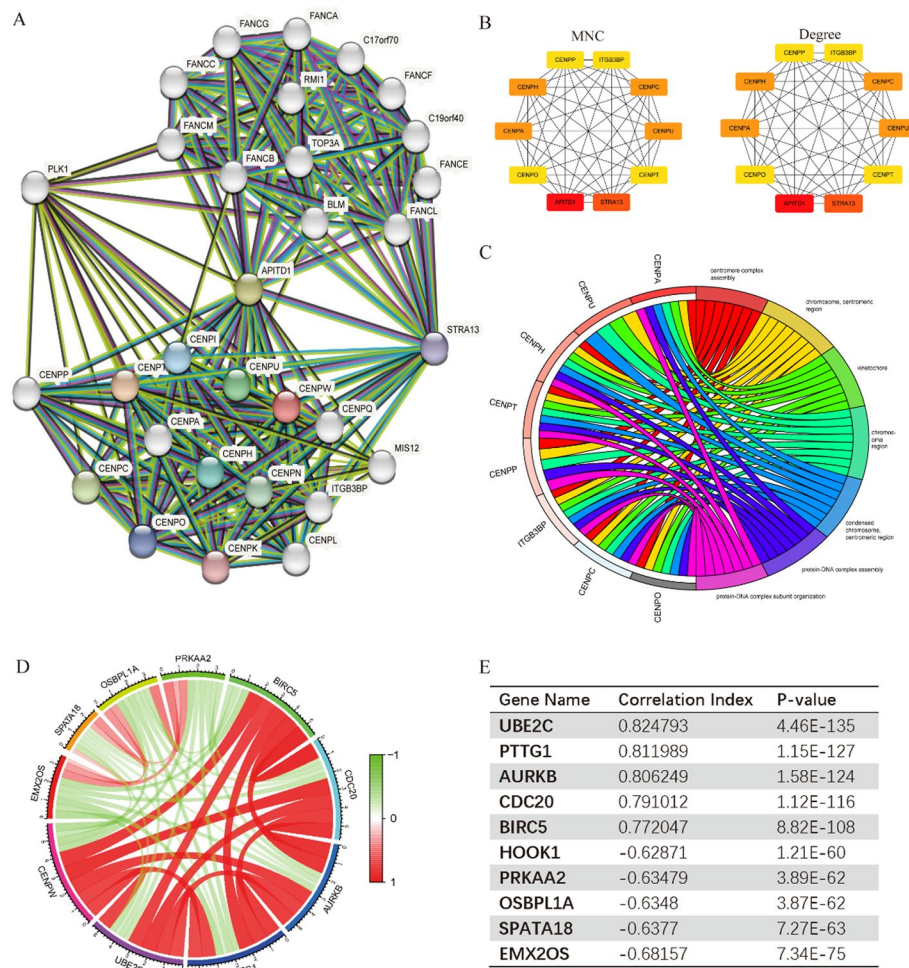


Fig. 4 The PPI network analysis and co-expression analysis of CENPW. **a** The PPI network of CENPW based on the STRING database. **b** The hubgene of the PPI network identified by MNC and Degree methods. **c** GO enrichment analysis of hubgene. **d, e** Top 10 co-expression genes of CENPW in TCGA-KIRC dataset

primarily interacts with genes related to DNA replication and cell division, thereby promoting the proliferation of ccRCC cells. The co-expressed genes with CENPW were determined based on Spearman correlation analysis across the whole transcriptome sequences of TCGA-KIRC. These are the top five positively correlated genes based on correlation coefficients (UBE2C, PTTG1, AURKB, CDC20, BIRC5) and the top 5 negatively correlated genes (HOOK1, PRKAA2, OSBPL1A, SPATA18, EMX2OS) were selected under the criterion of P-value less than 0.01.

3.6 CENPW is involved in immune cell infiltration of ccRCC

GO enrichment analysis data pointed out that CENPW may be involved in tumor immunology. Given that tumor immune cell infiltration is essential in tumor development, CENPW and immune infiltration need to be investigated.

First, the TIMER database was used to analyze the correlation between CENPW expression and immune cell infiltration. A negative association was seen between the expression of CENPW and tumor purity, whereas a positive correlation was found between CENPW expression with the quantification of CD8+ cells, CD4+ T cells, B cells, Neutrophils, Macrophages, and Dendritic cells infiltrating the tumor (Fig. 5a).

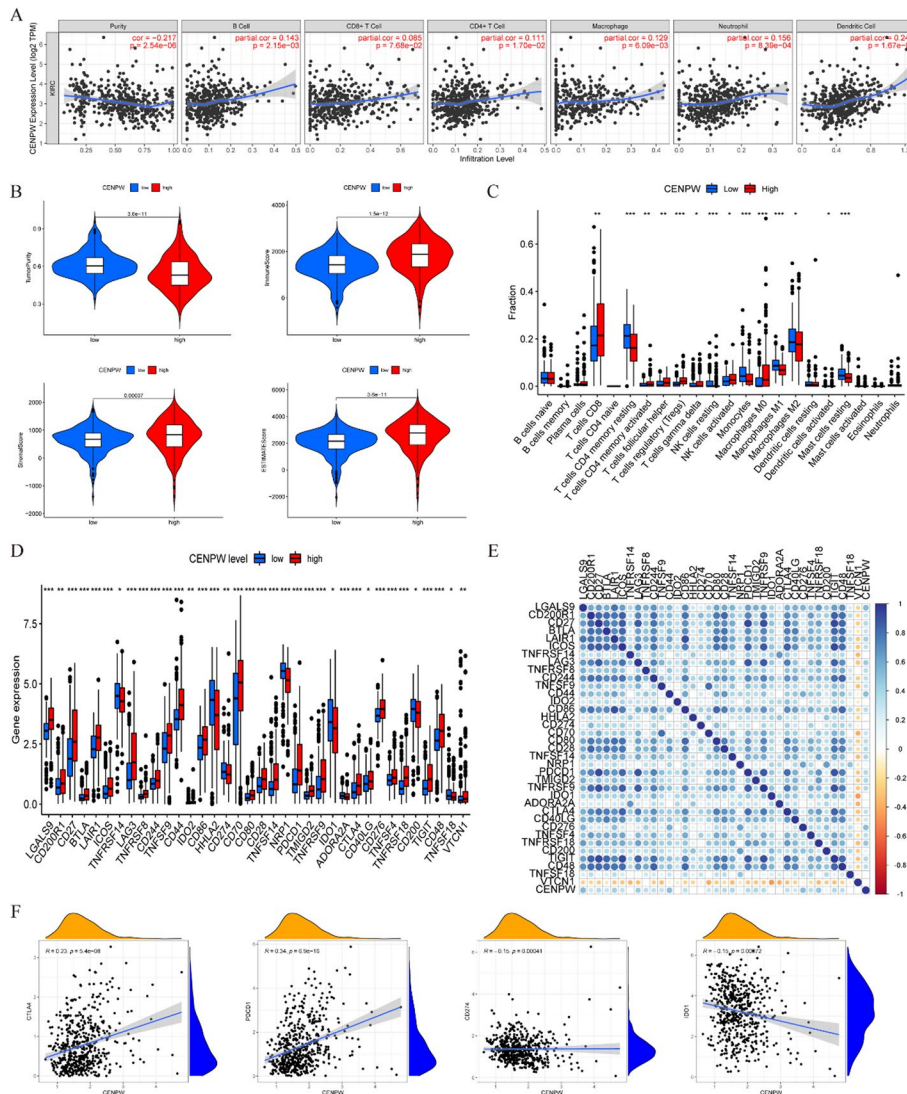


Fig. 5 Immune infiltration and immune checkpoint analysis of CENPW. **a** The correlation between CENPW expression with tumor purity and immune cells based on the TIMER database. **b** ESTIMATE analysis of TME differences between two groups. **c** Immune cell infiltration differences between CENPW high-expression and CENPW low-expression groups. **d** The expression levels of immune checkpoints between CENPW high-expression and CENPW low-expression groups. **e, f** The correlation between the expression level of CENPW and common immune checkpoints

Then, the ESTIMATE algorithm, applied to TCGA-KIRC expression data, assessed differences in tumor-associated stromal and immune cell infiltration between high and low CENPW expression groups. Consistent with TIMER findings, tumor purity was significantly reduced in the CENPW high-expression group, which exhibited greater abundance of immune and stromal cells. The Immune Score, Stromal Score, and comprehensive ESTIMATE Score were all significantly higher in the high CENPW expression group compared to the low-expression group (Fig. 5b).

Next, to supplement TIMER data, CIBERSORT algorithms were employed to compare immune cell infiltration between the two groups. Consistent with Fig. 5a, CD8+ T cells and M0 macrophages showed higher infiltration in the CENPW high-expression group.

Additionally, increased infiltration of activated follicular helper T cells, memory CD4+ T cells, NK cells, $\gamma\delta$ T cells, and dendritic cells was observed in this group (Fig. 5c).

At last, as immune checkpoint therapy has become increasingly important in cancer therapy, an exploration of the co-relation between immune checkpoints and CENPW expression is necessary. It founded out that 27 immune checkpoints were elevated in the CENPW high-expressed group and were positively associated with CENPW expression level to varying degrees (Fig. 5d, e). CTLA4, a target of Ipilimumab for immunotherapy, was associated with the expression level of CENPW. Another gene, PDCD1 encoding PD1 showed positive correlations with CENPW expression. Conversely, CD274 (PD-L1) and IDO1 were negatively correlated with CENPW expression (Fig. 5f).

3.7 Immunotherapy and chemotherapy responsibility of CENPW

To better evaluate the value of immune checkpoint inhibitors targeting CTLA4 and PD1 and find potential chemotherapy molecules for ccRCC, the authors performed immunophenoscore (IPS) analysis and IC50 analysis based on the TCIA database and the ‘pRRophetic’ R package. The results revealed that the CENPW high-expressed group showed greater IPS-CTLA4-pos-PD1-neg and IPS-CTLA4-pos-PD1-pos values but Statistical analysis did not reveal a significant difference between the IPS-CTLA4_neg_PD1_pos and IPS-CTLA4_neg_PD1_neg values (Fig. 6a), which indicates that high CENPW group responded better to CTLA4 inhibitor alone or CTLA4 inhibitor combined with PD-1 inhibitor. Patients with high CENPW expression may exhibit greater sensitivity to CTLA4 inhibitor treatment. Additionally, these patients were more susceptible

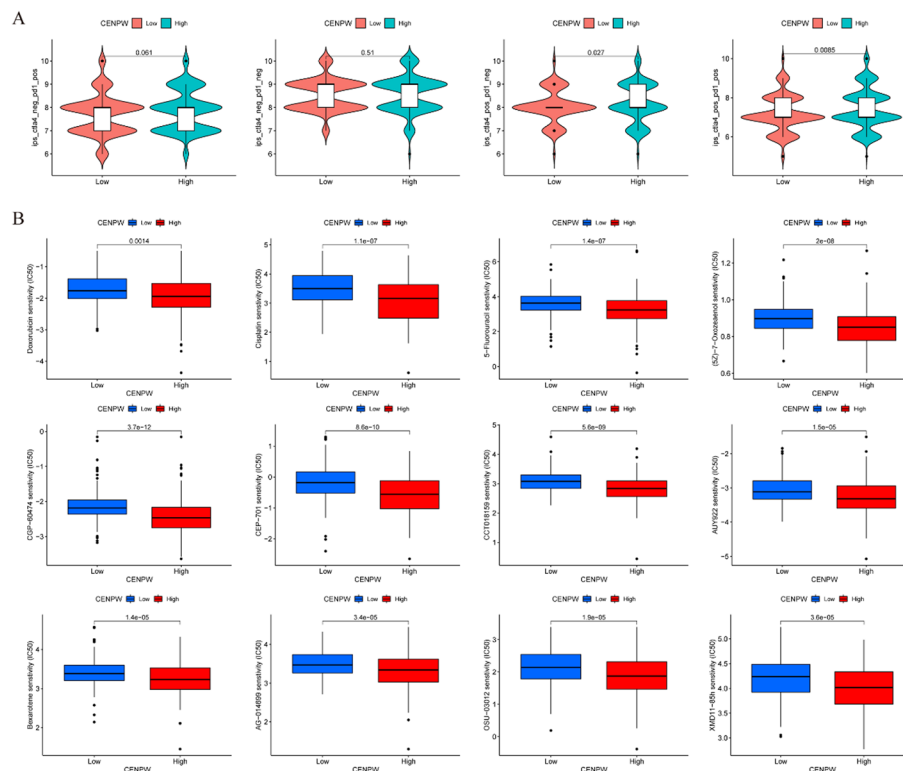


Fig. 6 Response to chemotherapy and immunotherapy between CENPW high-expression and CENPW low-expression groups. **a** Response to CTLA-4 and PD-1 inhibitors in the CENPW high-expression and CENPW low-expression groups. **b** Sensitivity of several chemotherapeutic molecules in the CENPW high-expression and CENPW low-expression groups

to first-line chemotherapy drugs, including 5-Fluorouracil, Cisplatin, and Doxorubicin. In addition, the authors also found other candidate drugs for high CENPW expression patients (Fig. 6b).

3.8 Verification of the function of CENPW in ccRCC

The authors also identified the expression level of CENPW in several renal cell carcinoma cell lines and selected 786-O and CAKI-1 cell lines, which were highly expressed CENPW compared to other cancer cells, for further experimental verification (Fig. 7a). After knocking down the expression of CENPW by siRNA (Fig. 7b), the cell viability (Fig. 7c), migration, and invasion abilities (Fig. 7d) were significantly reduced.

3.9 CENPW regulates lipid metabolism in ccRCC

Through GO pathway enrichment analysis of the CENPW dataset, we found that CENPW might be associated with lipoprotein activity, which can enhance the uptake of lipid synthesis precursors through the cell membrane. This activity could contribute

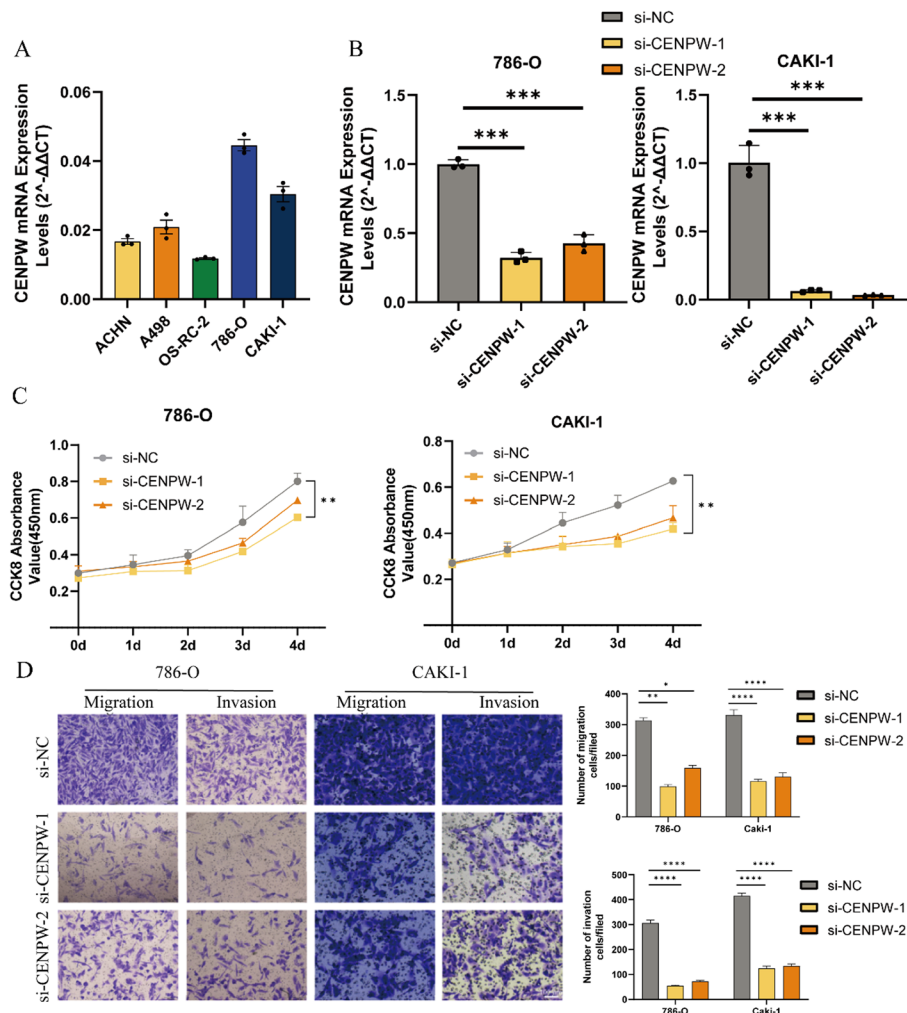


Fig. 7 Inhibit CENPW expression affects renal cell carcinoma cell proliferation, migration, and invasion. **a** qRT-PCR analysis of CENPW expression in renal cell carcinoma cell lines. **b** Knocked down the expression of CENPW in 786-O and Caki-1 cell lines. **c** Knocked down the expression of CENPW regressed the proliferation ability of renal cell carcinoma cells. **d** Knocked down the expression of CENPW inhibits renal cell carcinoma cell migration and invasion

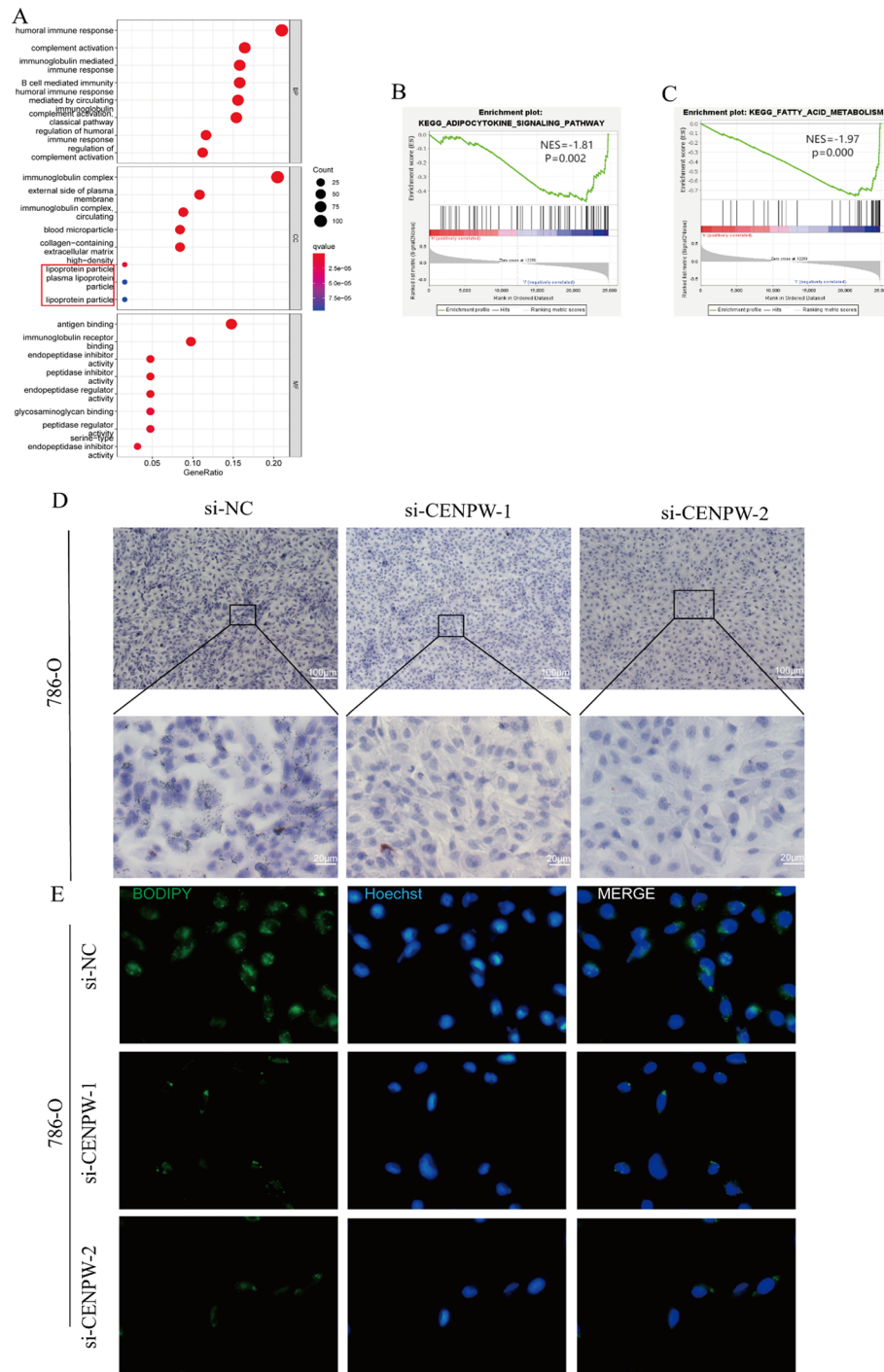


Fig. 8 GO Enrichment analysis of CENPW in ccRCC. **a** Gene set enrichment analysis (GSEA) of CENPW in ccRCC. **b**, **c** The Oil Red O staining experiment revealed changes in lipid droplet content in 786-O cells when the expression level of CENPW decreased. **d** BODIPY 493/503 staining demonstrated changes in lipid droplet content

to the accumulation of lipid droplets in ccRCC (Fig. 8. a). GSEA enrichment analysis revealed that high CENPW is highly expressed, the adipocytokine signaling pathway and fatty acids metabolism are activated, thus regulating lipid metabolism in ccRCC (Fig. 8b, c). To investigate the functional impact of CENPW on lipid metabolism in ccRCC, we performed an Oil Red O staining experiment (Fig. 8d). The results showed that knocking

down CENPW significantly reduced lipid droplet accumulation in the 786-O cell line. Then, we conducted BODIPY 493/503 staining on 786-O cells and observed that neutral lipid droplets in renal cell carcinoma were markedly reduced after CENPW knockdown (Fig. 8e). Therefore, CENPW plays a pivotal role in regulating lipid droplet content in ccRCC.

4 Discussion

The treatment of ccRCC is still difficult considering the high metastasis rate and chemoresistance occurrence, so the discovery of biomarkers for early diagnosis and targeted therapies is of great importance [17]. Advances in next-generation sequencing (NGS) have significantly facilitated the identification of novel biomarkers. For instance, Pu et al. identified TREM-1 as a potential diagnostic biomarker for ccRCC, which was also linked to immune infiltration through bioinformatics analysis [18]. In this study, the author identified CENPW as a biomarker and therapeutic target for ccRCC. CENPW expression is significantly higher in tumor tissues compared to normal tissues through analyses of the TCGA and GEO databases. High CENPW expression was associated with tumor progression and poor survival outcomes, as shown in the TCGA-KIRC database. Enrichment analyses (KEGG, GO, and GSEA) suggested that CENPW is linked to pathways such as fat digestion, absorption, and cytokine receptor interaction. In vitro experiments confirmed that CENPW expression is elevated in tumor tissues. Knockdown of CENPW in ccRCC cells inhibited proliferation, migration, and invasion, and reduced lipid droplet accumulation, as shown by Oil Red O and Bodipy 493/503 assays. In summary, CENPW plays a key role in ccRCC progression, with significant associations with immune cell infiltration and lipid metabolism. These findings highlight CENPW as a promising prognostic biomarker and therapeutic target for ccRCC.

CENPW, a key protein involved in the formation of centromeric nucleosomes [10], has been recognized to be upregulated in various cancers. Wang et al. reported the abnormal expression level of CENPW in breast cancer, and high expression of CENPW was correlated with adverse clinical features [19]. Similarly, this study revealed that CENPW was elevated in ccRCC patients based on various datasets and laboratory experiments, we found that the expression level of CENPW increases with the rise in tumor malignancy. This phenomenon is particularly evident in TNM staging and is also observed in histological grading and classification. The results also point out that patients with high expressions of CENPW have poor survival rates. Taken together, these results indicate that CENPW is an adverse factor to the patient's prognosis and may serve as a diagnostic therapeutic target and biomarker for ccRCC patients. Zhou et al. found that CENPW could promote hepatocellular carcinoma progression by activating the E2F signal pathway [9]. Still, the exact mechanism by which CENPW contributes to the malignancy of ccRCC remains unclear.

The most outstanding characteristic of ccRCC is the aberrant metabolic process reorganization to promote unbridled tumor growth [20–23]. Instead of extracting energy from mitochondrial oxidative phosphorylation and lipid decomposition [24–28], ccRCC cells rely on the glycolysis [26, 29, 30]. These lead to the remarkable lipid accumulation in the ccRCC. Lipid metabolic reprogramming plays a critical role in ccRCC, significantly impacting tumor initiation, progression, and malignant behavior [31]. Key characteristics of metabolic reprogramming in tumors include increased lipid storage,

alterations in fatty acid metabolism, and cholesterol metabolism dysregulation [32–34]. This reprogramming influences ccRCC progression by affecting tumor growth, migration, invasion, and immune evasion [35]. Li et al. discovered that CTBP1-DT regulates lipid synthesis in clear cell renal cell carcinoma (ccRCC), thereby promoting the progression of renal cancer [36]. In another research, an important regulator of lipid metabolism in ccRCC, the isoform of Annexin A3, was discovered [25]. In our study, we found the potential role of CENPW in regulating ccRCC lipid accumulation. Enrichment analysis revealed that CENPW regulates the adipocytokine signaling pathway and fatty acid metabolism, thereby contributing to lipid droplet accumulation in ccRCC. Furthermore, our experiments demonstrated that knocking down CENPW significantly reduces lipid droplets in clear cell renal cell carcinoma (ccRCC) cells. Since lipid droplets are critical substances in the development and progression of ccRCC, their significant reduction notably impacts tumor cell growth. However, the specific mechanisms by which CENPW influences lipid droplet synthesis remain to be elucidated.

Another unexpected finding is the underlying relationship between CENPW and immune cell infiltration. Clear cell renal cell carcinoma (ccRCC) is one of the most immune-infiltrated tumor types, characterized by a unique tumor microenvironment (TME) enriched with abundant immune cells yet exhibiting pronounced immunosuppressive properties [37–39]. Multiple regulators could influence the infiltration of immune cells, such as miR-29b and miR-198, which could induce CD8⁺ T cell dysfunction in ccRCC [40]. Through TIMER analysis, we found correlations between CENPW expression and immune cell infiltration, such as CD8⁺ T cells, CD4⁺ T cells, and B cells. These findings indicated the function of CENPW in tumor microenvironment regulation. Recently, emerging evidence also emphasizes the role of certain metabolic pathways in regulating tumor microenvironments, such as complements [41] and kynurenine [42]. As an important metabolic process, lipid metabolism could also influence the immune microenvironment in ccRCC. For instance, oxidized lipids could induce the immune dysfunction of CD8⁺ T cells [43]. In our study, CENPW was associated with immune cell infiltration and lipid metabolic signal pathways. We speculate that CENPW may also regulate immune cell activity by augmenting the lipid metabolism process, further research focusing on this mechanism would be significant.

Dysregulated tumor microenvironments could also affect the therapy responses of ccRCC [44–48]. Studies have shown that the expression levels of programmed death receptor-1 (PD-1), its ligand (PD-L1), and cytotoxic T-lymphocyte antigen-4 (CTLA4) are significantly elevated in tumor tissues of ccRCC patients [49]. Due to the pivotal roles of PD-L1 and CTLA4 in the TME, CTLA4, and PD-1/PD-L1 inhibitors have become mainstay treatments for ccRCC in recent years, particularly in advanced or metastatic cases [50]. Clinical studies have demonstrated that combination immunotherapy (e.g., Ipilimumab combined with Nivolumab) significantly improves overall survival and progression-free survival in ccRCC patients [51]. Our study reveals the multifaceted role of CENPW in influencing the treatment response of ccRCC. High CENPW expression level was correlated with the upregulation of 27 immune checkpoints, including CTLA4 and PDCD1. TCIA database analysis further showed that patients with high CENPW expression respond better to CTLA4 inhibitors and exhibit greater sensitivity to chemotherapy drugs like 5-fluorouracil, cisplatin, and doxorubicin. By modulating immune cell infiltration, cytokine signaling, immune checkpoint expression, and metabolic pathways,

CENPW emerges as a key driver of TME dynamics and tumor progression. Its association with immune checkpoint molecules, particularly CTLA4 and PD-1, underscores its potential as a predictive biomarker for immunotherapy response. These findings lay the theoretical groundwork for future exploration of CENPW's therapeutic value, whether through direct inhibition or by leveraging its role in TME metabolism-immune interactions for targeted interventions.

5 Conclusion

In conclusion, the authors investigated the role of CENPW in ccRCC. CENPW was upregulated in tumors compared to normal renal tissues. CENPW was also associated with worse clinical outcomes. In addition, CENPW was involved in immune cell infiltration and could serve as a potential target for immunotherapy and chemotherapy. Finally, by knocking down the expression of CENPW in RCC cells, the authors found that CENPW was associated with cancer cell viability, migration, and invasion abilities.

Abbreviations

ccRCC	Clear cell renal cell carcinoma
CENP-W	Centromere protein W
NCBI	National Center for Biotechnology Information
TCGA	The Cancer Genome Atlas
GSEA	Gene Set Enrichment Analysis
CAFs	Cancer-associated fibroblasts
CTLA4	Cytotoxic T-Lymphocyte Associated Protein 4
PDCD1	Programmed Cell Death 1
qRT-PCR	Real-time quantitative PCR
MNC	Maximum Neighborhood Component
UBE2C	Ubiquitin-Conjugating Enzyme E2 C
PTTG1	Tumor-Transforming Protein 1
AURKB	Aurora/IPL1-Related Kinase 2
CDC20	Cell Division Cycle Protein 20 Homolog
BIRC5	Baculoviral IAP Repeat Containing 5
HOOK1	Hook Homolog 1
PRKAA2	AMPK Subunit Alpha-2
OSBPL1A	Oxysterol Binding Protein Like 1A
SPATA18	Spermatogenesis Associated 18
EMX2OS	Empty Spiracles Homeobox 2 Opposite Strand

Acknowledgements

We express sincere appreciation to all the patients who took part in this study, for their invaluable contributions. Sincere appreciation to the experts and editors for making this study better.

Author contributions

XHB, FMT and LHL: conception and design this study; XQL, WBJ and GY: Gathering and assembling of data; XHB, XQL and WWK: analyzing and interpreting data; XHB and FMT: writing and reviewing manuscripts. Manuscript final approval: All authors.

Funding

This research was funded by the the Natural Science Research Project of Anhui Universities (2022AH051184).

Availability of data and materials

The datasets mainly include the following from the GEO database: GSE53757 (whole transcriptome analysis of RNA from tumor and normal tissues of patients) and GSE36895 (comparison of whole transcriptome analysis of tumor tissues from patients and subcutaneous tumor tissues from mice with normal renal epithelial tissues); from the TCGA database: TCGA-KIRC This study primarily collected datasets from three databases, namely GEO, TCGA, and TCIA. The datasets mainly include the following from the GEO database: GSE53757 (whole transcriptome analysis of RNA from tumor and normal tissues of patients) and GSE36895 (comparison of whole transcriptome analysis of tumor tissues from patients and subcutaneous tumor tissues from mice with normal renal epithelial tissues); from the TCGA database: TCGA-KIRC (which includes patient clinical information, such as TNM staging, pathological grade, age, gender, etc.); from the TCIA database: which includes immunophenoscore (IPS) analysis and IC50 analysis. The collected datasets from the databases were processed using RStudio to convert the expression matrices into differential gene datasets.(which includes patient clinical information, such as TNM staging, pathological grade, age, gender, etc.); from the TCIA database (<https://tcia.at/about>): which includes immunophenoscore (IPS) analysis and IC50 analysis. The collected datasets from the databases were processed using RStudio to convert the expression matrices into differential gene datasets.

Declarations

Ethics approval and consent to participate

The present investigation implemented the guidelines outlined in the Declaration of Helsinki and received approval from the Ethics Committee of Human Research at the First Affiliated Hospital of Anhui Medical University (PJ2019-14–22). Informed consent was obtained from all individual participants included in the study.

Competing interests

The authors declare no competing interests.

Received: 7 November 2024 / Accepted: 29 May 2025

Published online: 18 June 2025

References

- Znaor A, Lortet-Tieulent J, Laversanne M, Jemal A, Bray F. International variations and trends in renal cell carcinoma incidence and mortality. *Eur Urol*. 2015;67(3):519–30. <https://doi.org/10.1016/j.eururo.2014.10.002>.
- Sung H, et al. Global Cancer Statistics 2020: GLOBOCAN estimates of incidence and mortality worldwide for 36 cancers in 185 countries. *CA Cancer J Clin*. 2021;71(3):209–49. <https://doi.org/10.3322/caac.21660>.
- Siegel RL, Miller KD, Wagle NS, Jemal A. Cancer statistics, 2023. *CA Cancer J Clin*. 2023;73(1):17–48. <https://doi.org/10.3322/caac.21763>.
- Rini BI, Campbell SC, Escudier B. Renal cell carcinoma. *Lancet*. 2009;373(9669):1119–32. [https://doi.org/10.1016/S0140-6736\(09\)60229-4](https://doi.org/10.1016/S0140-6736(09)60229-4).
- Lee S, et al. Molecular cloning and functional analysis of a novel oncogene, cancer-upregulated gene 2 (CUG2). *Biochem Biophys Res Commun*. 2007;360(3):633–9. <https://doi.org/10.1016/j.bbrc.2007.06.102>.
- Kim H, Lee S, Park B, Che L, Lee S. Sp1 and Sp3 mediate basal and serum-induced expression of human CENP-W. *Mol Biol Rep*. 2010;37(7):3593–600. <https://doi.org/10.1007/s11033-010-0008-3>.
- Yawut N, et al. Translocalization of enhanced PKM2 protein into the nucleus induced by cancer upregulated gene 2 confers cancer stem cell-like phenotypes. *BMB Rep*. 2022;55(2):98–103. <https://doi.org/10.5483/BMBRep.2022.55.2.118>.
- Malilas W, et al. Cancer upregulated gene 2, a novel oncogene, enhances migration and drug resistance of colon cancer cells via STAT1 activation. *Int J Oncol*. 2013;43(4):1111–6. <https://doi.org/10.3892/ijo.2013.2049>.
- Zhou Y, et al. Knockdown of CENPW inhibits hepatocellular carcinoma progression by inactivating E2F signaling. *Technol Cancer Res Treat*. 2021;20:15330338211007252. <https://doi.org/10.1177/15330338211007253>.
- Kaowinn S, Yawut N, Koh SS, Chung Y-H. Cancer upregulated gene (CUG)2 elevates YAP1 expression, leading to enhancement of epithelial-mesenchymal transition in human lung cancer cells. *Biochem Biophys Res Commun*. 2019;511(1):122–8. <https://doi.org/10.1016/j.bbrc.2019.02.036>.
- Prendergast L, et al. The CENP-T/-W complex is a binding partner of the histone chaperone FACT. *Genes Dev*. 2016;30(11):1313–26. <https://doi.org/10.1101/gad.275073.115>.
- Zhang P, et al. CENPW knockdown inhibits progression of bladder cancer through inducing cell cycle arrest and apoptosis. *J Cancer*. 2024;15(3):858–70. <https://doi.org/10.7150/jca.90449>.
- Zhou Z, Zhou Z, Huang Z, He S, Chen S. Histone-fold centromere protein W (CENP-W) is associated with the biological behavior of hepatocellular carcinoma cells. *Bioengineered*. 2020;11(1):729–42. <https://doi.org/10.1080/21655979.2020.1787776>.
- Gonzalez H, Hagerling C, Werb Z. Roles of the immune system in cancer: from tumor initiation to metastatic progression. *Genes Dev*. 2018;32(19–20):1267–84. <https://doi.org/10.1101/gad.314617.118>.
- Wei SC, Duffy CR, Allison JP. Fundamental mechanisms of immune checkpoint blockade therapy. *Cancer Discov*. 2018;8(9):1069–86. <https://doi.org/10.1158/2159-8290.CD-18-0367>.
- Manguso RT, et al. In vivo CRISPR screening identifies Ptpn2 as a cancer immunotherapy target. *Nature*. 2017;547(7664):413–8. <https://doi.org/10.1038/nature23270>.
- Schiavoni V, et al. Recent advances in the management of clear cell renal cell carcinoma: novel biomarkers and targeted therapies. *Cancers*. 2023;15(12):3207. <https://doi.org/10.3390/cancers15123207>.
- TREM-1 as a potential prognostic biomarker associated with immune infiltration in clear cell renal cell carcinoma. <https://pubmed.ncbi.nlm.nih.gov/37217993/>. Accessed 25 Aug 2024.
- Wang L, et al. Investigating CENPW as a novel biomarker correlated with the development and poor prognosis of breast carcinoma. *Front Genet*. 2022;13: 900111. <https://doi.org/10.3389/fgene.2022.900111>.
- di Meo NA, et al. The dark side of lipid metabolism in prostate and renal carcinoma: novel insights into molecular diagnostic and biomarker discovery. *Expert Rev Mol Diagn*. 2023;23(4):297–313. <https://doi.org/10.1080/14737159.2023.2195553>.
- Lucarelli G, et al. Metabolomic insights into pathophysiological mechanisms and biomarker discovery in clear cell renal cell carcinoma. *Expert Rev Mol Diagn*. 2019;19(5):397–407. <https://doi.org/10.1080/14737159.2019.1607729>.
- di Meo NA, et al. Renal cell carcinoma as a metabolic disease: an update on main pathways, potential biomarkers, and therapeutic targets. *Int J Mol Sci*. 2022;23(22):14360. <https://doi.org/10.3390/ijms232214360>.
- De Marco S, et al. The cross-talk between Abl2 tyrosine kinase and TGFβ1 signalling modulates the invasion of clear cell renal cell carcinoma cells. *FEBS Lett*. 2023;597(8):1098–113. <https://doi.org/10.1002/1873-3468.14531>.
- Lucarelli G, et al. Integrated multi-omics characterization reveals a distinctive metabolic signature and the role of NDU-FA4L2 in promoting angiogenesis, chemoresistance, and mitochondrial dysfunction in clear cell renal cell carcinoma. *Aging*. 2018;10(12):3957–85. <https://doi.org/10.18632/aging.101685>.
- Bombelli S, et al. 36-kDa Annexin A3 isoform negatively modulates lipid storage in clear cell renal cell carcinoma cells. *Am J Pathol*. 2020;190(11):2317–26. <https://doi.org/10.1016/j.ajpath.2020.08.008>.
- Bianchi C, et al. The glucose and lipid metabolism reprogramming is grade-dependent in clear cell renal cell carcinoma primary cultures and is targetable to modulate cell viability and proliferation. *Oncotarget*. 2017;8(69):113502–15. <https://doi.org/10.18632/oncotarget.23056>.

27. Lucarelli G, et al. MUC1 tissue expression and its soluble form CA15-3 identify a clear cell renal cell carcinoma with distinct metabolic profile and poor clinical outcome. *Int J Mol Sci.* 2022;23(22):13968. <https://doi.org/10.3390/ijms232213968>.
28. Milella M, et al. The role of MUC1 in renal cell carcinoma. *Biomolecules.* 2024;14(3):315. <https://doi.org/10.3390/biom14030315>.
29. Ragone R, et al. Renal cell carcinoma: a study through NMR-based metabolomics combined with transcriptomics. *Diseases.* 2016;4(1):7. <https://doi.org/10.3390/diseases4010007>.
30. Metabolomic profile of glycolysis and the pentose phosphate pathway identifies the central role of glucose-6-phosphate dehydrogenase in clear cell-renal cell carcinoma. <https://pubmed.ncbi.nlm.nih.gov/25945836/>. Accessed 20 Mar 2025.
31. Sainero-Alcolado L, et al. Targeting MYC induces lipid droplet accumulation by upregulation of HILPDA in clear cell renal cell carcinoma. *Proc Natl Acad Sci USA.* 2024;121(7):e2310479121. <https://doi.org/10.1073/pnas.2310479121>.
32. Xiao H, et al. HIF-2 α /LINC02609/APOL1-mediated lipid storage promotes endoplasmic reticulum homeostasis and regulates tumor progression in clear-cell renal cell carcinoma. *J Exp Clin Cancer Res.* 2024;43:29. <https://doi.org/10.1186/s13046-023-02940-6>.
33. Hua X, et al. MED15 is upregulated by HIF-2 α and promotes proliferation and metastasis in clear cell renal cell carcinoma via activation of SREBP-dependent fatty acid synthesis. *Cell Death Discov.* 2024;10(1):188. <https://doi.org/10.1038/s41420-024-01944-1>.
34. Fei M, et al. HIF-2 α /LPCAT1 orchestrates the reprogramming of lipid metabolism in ccRCC by modulating the FBXW7-mediated ubiquitination of ACLY. *Int J Biol Sci.* 2025;21(2):614–31. <https://doi.org/10.7150/ijbs.103032>.
35. Manzo T, et al. Accumulation of long-chain fatty acids in the tumor microenvironment drives dysfunction in intrapancreatic CD8+ T cells. *J Exp Med.* 2020;217(8):e20191920. <https://doi.org/10.1084/jem.20191920>.
36. Li H, et al. Identify CTBP1-DT as an immunological biomarker that promotes lipid synthesis and apoptosis resistance in KIRC. *Gene.* 2024;914: 148403. <https://doi.org/10.1016/j.gene.2024.148403>.
37. Vuong L, Kotecha RR, Voss MH, Hakimi AA. Tumor microenvironment dynamics in clear-cell renal cell carcinoma. *Cancer Discov.* 2019;9(10):1349–57. <https://doi.org/10.1158/2159-8290.CD-19-0499>.
38. Tamma R, et al. Microvascular density, macrophages, and mast cells in human clear cell renal carcinoma with and without bevacizumab treatment. *Urol Oncol.* 2019;37(6):355.e11-355.e19. <https://doi.org/10.1016/j.urolonc.2019.01.025>.
39. Sjöberg E. Molecular mechanisms and clinical relevance of endothelial cell cross-talk in clear cell renal cell carcinoma. *Ups J Med Sci.* 2024. <https://doi.org/10.48101/ujms.v129.10632>.
40. Gigante M, et al. miR-29b and miR-198 overexpression in CD8+ T cells of renal cell carcinoma patients down-modulates JAK3 and MCL-1 leading to immune dysfunction. *J Transl Med.* 2016;14:84. <https://doi.org/10.1186/s12967-016-0841-9>.
41. Netti GS, et al. PTX3 modulates the immunoflogosis in tumor microenvironment and is a prognostic factor for patients with clear cell renal cell carcinoma. *Aging.* 2020;12(8):7585–602. <https://doi.org/10.18632/aging.103169>.
42. Lucarelli G, et al. Activation of the kynurenine pathway predicts poor outcome in patients with clear cell renal cell carcinoma. *Urol Oncol.* 2017;35(7):461.e15-461.e27. <https://doi.org/10.1016/j.urolonc.2017.02.011>.
43. Jin H-R, et al. Lipid metabolic reprogramming in tumor microenvironment: from mechanisms to therapeutics. *J Hematol Oncol.* 2023;16(1):103. <https://doi.org/10.1186/s13045-023-01498-2>.
44. Lasorsa F, et al. Complement system and the kidney: its role in renal diseases, kidney transplantation and renal cell carcinoma. *Int J Mol Sci.* 2023;24(22):16515. <https://doi.org/10.3390/ijms242216515>.
45. Lasorsa F, et al. Immune checkpoint inhibitors in renal cell carcinoma: molecular basis and rationale for their use in clinical practice. *Biomedicines.* 2023;11(4):1071. <https://doi.org/10.3390/biomedicines11041071>.
46. Ghini V, et al. Metabolomics to assess response to immune checkpoint inhibitors in patients with non-small-cell lung cancer. *Cancers.* 2020;12(12):3574. <https://doi.org/10.3390/cancers12123574>.
47. Lucarelli G, et al. MUC1 expression affects the immunoflogosis in renal cell carcinoma microenvironment through complement system activation and immune infiltrate modulation. *Int J Mol Sci.* 2023;24(5):4814. <https://doi.org/10.3390/ijms24054814>.
48. Lasorsa F, et al. Cellular and molecular players in the tumor microenvironment of renal cell carcinoma. *J Clin Med.* 2023;12(12):3888. <https://doi.org/10.3390/jcm12123888>.
49. Monjaras-Avila CU, Lorenzo-Leal AC, Luque-Badillo AC, D'Costa N, Chavez-Muñoz C, Bach H. The tumor immune microenvironment in clear cell renal cell carcinoma. *Int J Mol Sci.* 2023;24(9):7946. <https://doi.org/10.3390/ijms24097946>.
50. Meng L, et al. Emerging immunotherapy approaches for advanced clear cell renal cell carcinoma. *Cells.* 2023;13(1):34. <https://doi.org/10.3390/cells13010034>.
51. Chen Y-W, Rini BI, Beckermann KE. Emerging targets in clear cell renal cell carcinoma. *Cancers.* 2022;14(19):4843. <https://doi.org/10.3390/cancers14194843>.

Publisher's Note

Springer Nature remains neutral with regard to jurisdictional claims in published maps and institutional affiliations.